

RESEARCH ARTICLE

FOCUS SHAPING OF CYLINDRICALLY POLARIZED VORTEX BEAMS BY A LINEAR AXICON

A. A. AlKelly^{1,*} , Ibrahim G. H. Loqman¹ , Hassan T. Al-Ahsab^{1,2} ¹ Physics Department, Faculty of Science, Sana'a University, Sana'a, Yemen² Physics Department, Faculty of Applied Science, Thamar University, Thamar, Yemen

*Corresponding author: A. A. AlKelly; Email: aa_alkelly@yahoo.com; Phone number: +967777267057

Received: 08 September 2021 / Accepted: 27 September 2021 / Published online: 31 December 2021

Abstract

Focus shaping of cylindrically polarized vortex beams (CPVBs) by linear axicon is studied theoretically. Vector diffraction theory has been used to derive the expressions of the light field in the focal region. It is shown that a different intensity distribution in the focal region can be obtained by adjusting the topological charge, the polarization rotation angle and the numerical aperture maximal angle. A focal spot, a dark channel and a flat-topped shapes are formed by choosing proper values of parameters. A controllable polarization state of dark channel is obtained. The different focal region shapes may find wide applications such as material processing and optical tweezers.

Keywords: Focus shaping, Polarization, Vortex beams, Linear axicon.

1. Introduction:

In recent years, vortex beams have attracted a lot of researchers attention due to their unique properties and wide applications. They possess a null intensity at the center along the optical axis due to phase singularities and a helical phase structure of $\exp(il\varphi)$, where l is the topological charge and φ is the polar coordinate in the plane perpendicular to the optical axis [1-5]. In addition to phase singularities, there are different types of polarization singularities such as radial polarization, azimuthal polarization and circular polarization. Laser beams that have both phase and polarization singularities have been successfully used in different applications such as optical manipulation of particles, particle acceleration, optical communication, lithography, and material processing [6-10].

Focusing of CPVBs have attracted a great attention of researchers interest due to their unique special properties [5, 11]. For instance, focusing radially polarized vortex beams can produce a very strong longitudinal electric field in the focal region and a sub-wavelength focal spot [7] and azimuthal polarized vortex beam can present hollow focus on the position of optical axis in focal plane [12]. In addition, the azimuthal polarization can be convert into the radial polarization, or vice versa [9]. Recently, focus shaping of CPVBs have been studied [10, 13-16]. To the best of our knowledge, the previous studies have been discussed focusing CPVBs by spherical lens. However, there is no studies on focusing

CPVBs by axicons; although, they are the most efficient optical elements that generate beams with large focal depth. Therefore, in this article, we will discuss the focus shaping of CPVBs by linear axicon.

In this article, focus shaping of CPVBs through linear axicon are numerically investigated in detail. The theoretical model are introduced in section 2. In section 3, the numerical results and discussions are shown. The results are concluded in section 4.

2. Theoretical Model

The scheme of optical system is shown in Fig.1, the axicon put on the optical aperture that its reduce ρ_p , the electric field of CPVBs will be considered incident on a linear axicon to which the transmittance is defined as $T(\rho) = \exp(ib\rho)$ where b is the axicon parameter that indicates the strength of the axicon which can be rewritten as [17]:

$$T = \exp(ib\rho) = \exp\left(ib\rho_p \cdot \frac{\rho}{\rho_p}\right) = \exp\left(ib\rho_p \cdot \frac{\rho/f}{\rho_p/f}\right) = \exp\left(iB \frac{\sin\theta}{NA}\right), \quad (1)$$

where $B = b\rho_p$ is the dimensionless axicon parameter, NA is the numerical aperture and θ denotes the tangential angle with respect to the z axis.

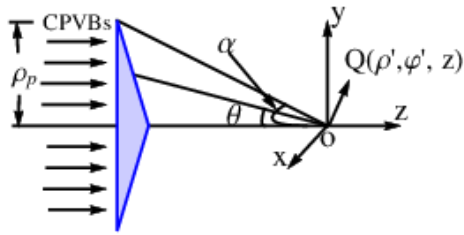


Fig 1. Scheme of optical system

According to vector diffraction theory, the electric field of the cylindrically polarized vortex beam in the focal region can be written as [18, 19]:

$$E(\rho', \phi', z) = E_{\rho'} e_{\rho'} + E_{\phi'} e_{\phi'} + E_z e_z, \quad (2)$$

where $e_{\rho'}$, $e_{\phi'}$ and e_z are the unit vectors in the radial, azimuthal and longitudinal directions, respectively. $E_{\rho'}$, $E_{\phi'}$ and E_z are the amplitude of the three orthogonal component that can be expressed as:

$$E_{\rho'}(\rho', \phi', z) = -\frac{iA}{2\pi} \cos\phi_0 \int_0^\alpha \int_0^{2\pi} \sqrt{\cos\theta} \sin 2\theta T(\theta) P(\theta) \cos(\phi - \phi') \exp[i\ell\phi] \times \exp[ik(z \cos\theta + \rho' \sin\theta \cos(\phi - \phi'))] d\phi d\theta, \quad (3)$$

$$E_{\phi'}(\rho', \phi', z) = -\frac{iA}{\pi} \sin\phi_0 \int_0^\alpha \int_0^{2\pi} \sqrt{\cos\theta} \sin\theta T(\theta) P(\theta) \cos(\phi - \phi') \exp[i\ell\phi] \times \exp[ik(z \cos\theta + \rho' \sin\theta \cos(\phi - \phi'))] d\phi d\theta, \quad (4)$$

$$E_z(\rho', \phi', z) = \frac{iA}{\pi} \cos\phi_0 \int_0^\alpha \int_0^{2\pi} \sqrt{\cos\theta} \sin^2\theta T(\theta) P(\theta) \exp[i\ell\phi] \times \exp[ik(z \cos\theta + \rho' \sin\theta \cos(\phi - \phi'))] d\phi d\theta, \quad (5)$$

where ρ' , ϕ' and z are the radial, azimuthal and longitudinal coordinates of observation point in the focal

3. Numerical Results and Discussion

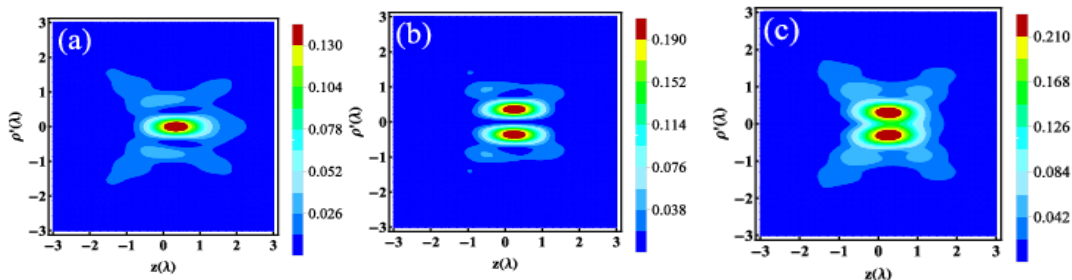


Fig 2. (a)-(c) Intensity distribution of CPVBs in the focal region for radially polarized vortex beams that corresponding to $\phi_0=0$ under condition $l=1$, $B=2$ and $\alpha=80^\circ$.

For all numerical calculation in this paper, it was supposed that $A=1$, $P(\theta)=1$ and $\lambda=632.8\text{nm}$. The length unit in all figures is the wavelength of the incident beam in vacuum and the polarization rotation angle will be changed from 0 to $\pi/2$. All the numerical results have been evaluated by using Mathematica 9.0.

region, respectively. θ denotes the tangential angle with respect to the z axis, ϕ is the azimuthal angle with respect to x axis, k is the wave number and $\alpha = \arcsin(NA)$ is the convergence angle corresponding to the radius of the incident optical aperture. Using the following formulae

$$\int_0^{2\pi} \exp[im\phi + it\cos(\phi - \phi')] d\phi = 2\pi i^m \exp(im\phi') J_m(t), \quad (6)$$

and

$$\int_0^{2\pi} \cos(\phi - \phi') \exp[im\phi + it\cos(\phi - \phi')] d\phi = i^{m+1} \exp(im\phi') [J_{m+1}(t) - J_{m-1}(t)]. \quad (7)$$

Therefore, the formulae of three orthogonal component of the electric field in the focal region are given by

$$E_{\rho'}(\rho', \phi', z) = \frac{i^\ell A}{2} \exp(i\ell\phi') \cos\phi_0 \int_0^\alpha \sqrt{\cos\theta} \sin 2\theta \exp\left(iB \frac{\sin\theta}{NA}\right) P(\theta) \times \exp[ik(z \cos\theta)] [J_{\ell+1}(k\rho' \sin\theta) - J_{\ell-1}(k\rho' \sin\theta)] d\theta, \quad (8)$$

$$E_{\phi'}(\rho', \phi', z) = i^\ell A \exp(i\ell\phi') \sin\phi_0 \int_0^\alpha \sqrt{\cos\theta} \sin\theta \exp\left(iB \frac{\sin\theta}{NA}\right) P(\theta) \times \exp[ikz \cos\theta] [J_{\ell+1}(k\rho' \sin\theta) - J_{\ell-1}(k\rho' \sin\theta)] d\theta, \quad (9)$$

and

$$E_z(\rho', \phi', z) = 2i^{\ell+1} A \exp(i\ell\phi') \cos\phi_0 \int_0^\alpha \sqrt{\cos\theta} \sin^2\theta \exp\left(iB \frac{\sin\theta}{NA}\right) P(\theta) \times \exp[ikz \cos\theta] J_\ell(k\rho' \sin\theta) d\theta, \quad (10)$$

where $J_{\ell-1}$, J_ℓ and $J_{\ell+1}$ are the Bessel function of the first kind with order $\ell - 1$, ℓ and $\ell + 1$, respectively. The intensity distribution corresponding to different component ($E_{\rho'}$, $E_{\phi'}$, E_z) and the total intensity in the focal region can be calculated by Eqs. 8–10.

Fig. 2 illustrates the numerical results of intensity distribution in the focal region for $\alpha=80^\circ$, $l=1$, $B=2$ and $\phi_0=0$ which is corresponding to radially polarized incident beam. It is shown from Fig. 2-(a) the radial component distribution is formed a focal spot with focus size i.e. full-width at half-maximum (FWHM) 0.433λ with maximum value 0.152a.u. at on-axis maximum point $z=0.334\lambda$, for this case i.e. the topological charge

$l=1$, the longitudinal component distribution is formed a focal hole with a dark spot size 0.173λ Fig. 2-(b). The azimuthal component distribution is vanishing.

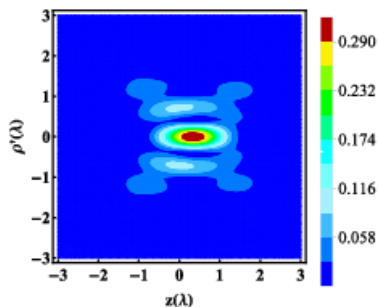
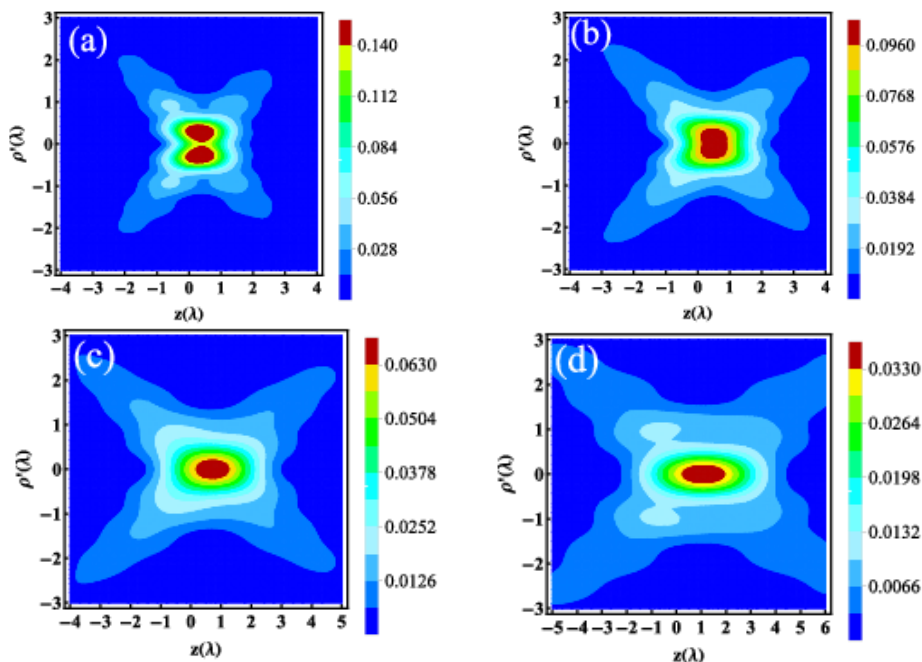


Fig 3. Intensity distribution of CPVBs in the focal region corresponding to $\varphi_0=90^\circ$ the other parameters are the same as those in Fig. 2.

These results clearly understood by analyzing the Bessel functions in Eqs. 8-10. Fig. 2-(c) shows the total intensity distribution in the focal region with FWHM 0.547λ and focal depth 1.56λ . Fig. 3 shows the intensity distribution in the focal region for $\varphi_0=90^\circ$, which is corresponding to azimuthally polarized incident beam. The maximum value of the intensity distribution equals 0.373a.u. that located at $z=0.30\lambda$. Its focal spot (FWHM) and focal depth are 0.40λ and 1.33λ , respectively. It is shown that both radial and azimuthal components are vanishing and the total intensity distribution has a maximum value 0.373a.u. on the optical axis at $z=0.30\lambda$ which construct



a highly confined focal spot with spot size 0.40λ .

Fig 4. Total intensity distribution of CPVBs in the focal region under condition of $l=1, B=2$ and $\varphi_0=0$ with a) $\alpha=70^\circ$, b) $\alpha=60^\circ$, c) $\alpha=50^\circ$ and d) $\alpha=40^\circ$.

A flat-topped total intensity distribution can be achieved when one, as shown in Fig. 4-(b), or two of intensity components have focal spot and the other one has a focal hole or vice versa under the condition that the size of the focal spot is similar to the size of the focal hole. Herein, it can be obtained by adjusting the value of the polarization rotation angle φ_0 of the optical vortex

beam and α . However, our results are agree with focus shaping of CPVBs by a high numerical aperture lens [13] the difference is that there is no a definite focus point instead of it there is a focal region that is extend along the optical axis z . The focal region is shifted either toward or outward the axicon lens on the optical axis depending on the value of axicon parameter and the maximal angle α .

Fig. 4 illustrate the intensity distribution of CPVBs under condition of $l=1, B=2$ and $\varphi_0=0$ for different values of α . It is shown that the shape of intensity distribution in the focal region changed and extended considerably on decreasing α and the maximum point shifted away from the axicon. It can be seen that the intensity on the optical axis becomes higher than the intensity around it when the values of α are decrease that's because the value of longitudinal component becomes higher than the radial component. It is shown from Fig. 4-(b) that a flat-topped total intensity distribution can be obtained when $\alpha=60^\circ$ with a flat-topped focus size FWHM (full-width at half-maximum) of the total intensity equals 1.22λ . It is clearly observed from Figs. 2-(c) and 4-(a)-(c) that the maximum value of the total intensity shifted away from the axicon and decreased with extending along the optical axis as the value of α decrease. There maximum values are $0.15, 0.136, 0.10, 0.07(\text{a.u.})$ at $z=0.33, 0.4, 0.51, 0.71(\lambda)$ that are corresponding to $\alpha=80, 70, 60, 50^\circ$, respectively. In addition, the corresponding focal depth are $1.57, 1.77, 2.20, 3(\lambda)$.

Fig. 5 illustrates the flat-topped total intensity distribution in the focal region for $B=3, B=4$ under condition $l=1, \varphi_0=0^\circ$ and $\alpha=60$. The flat topped focus size FWHM of the total intensity equals 1.16λ which is wider than that obtained when focusing CPVBs by a high numerical-aperture lens [12]. It indicates that linear axicon is appropriate for obtaining an idial flat-

topped focus. Moreover, the flat topped focus sizes are 1.18λ and 1.21λ for $\varphi_0=31^\circ, \alpha=75^\circ$ and $\varphi_0=28^\circ, \alpha=70^\circ$, respectively. It is found that the maxima of the intensity decreases as well as both α and processing, microlithography and improving printing filling factor.

φ_0 decrease. In the other hand the flat topped focus size increases. This flat-topped is may be useful in material

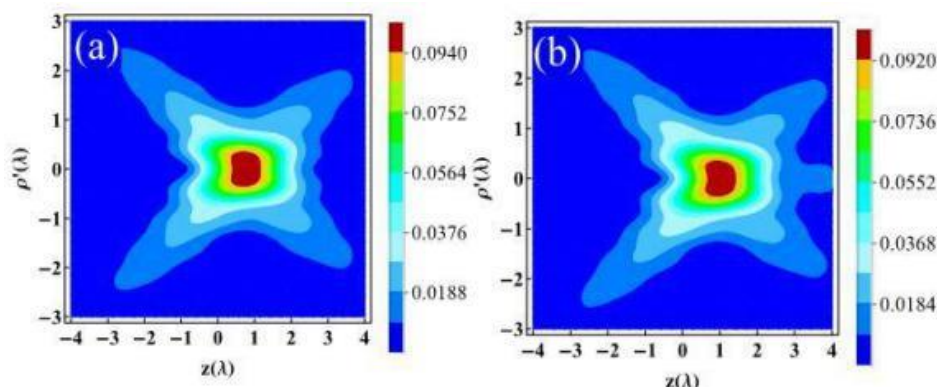


Fig 5. Total intensity distribution of CPVBs in the focal region under condition $l=1$, $\varphi_0=0^\circ$ and $\alpha=60^\circ$ with a) $B=3$ and b) $B=4$

We can note from Eqs. 8–10 that for $l=1, 0$ or -1 a nonzero intensity on the optical axis is obtained due to the presence of Bessel function of the zero-order. However, for all other topological charge a zero intensity on the optical axis, i.e. a dark channel along the optical axis, is obtained due to the destructive interference. Fig. 6 shows the total intensity distribution of focal hole $l=2$ with different values of φ_0 . The focal hole size is increasing as well as φ_0 decrease. It is 0.3λ at $z=0.33\lambda$ for azimuthally polarized vortex ($\varphi_0=90^\circ$) Figs. 6–(a) and 0.45λ for radially polarized vortex $\varphi_0=0^\circ$ Figs. 6–(d).

Moreover, a longitudinal polarized dark hollow channel is achieved at focal region when ($\varphi_0=0^\circ$) and azimuthal polarized dark hollow channel with a side lobes is achieved at the focal region when ($\varphi_0=90^\circ$). These side lobes are reduced as well as φ_0 decrease. In addition, it can be seen that by adjusting the value of φ_0 the polarization state of dark channel is changed considerably from azimuthally polarized when $\varphi_0=0$ to linearly polarized dark channel when $\varphi_0=90$.

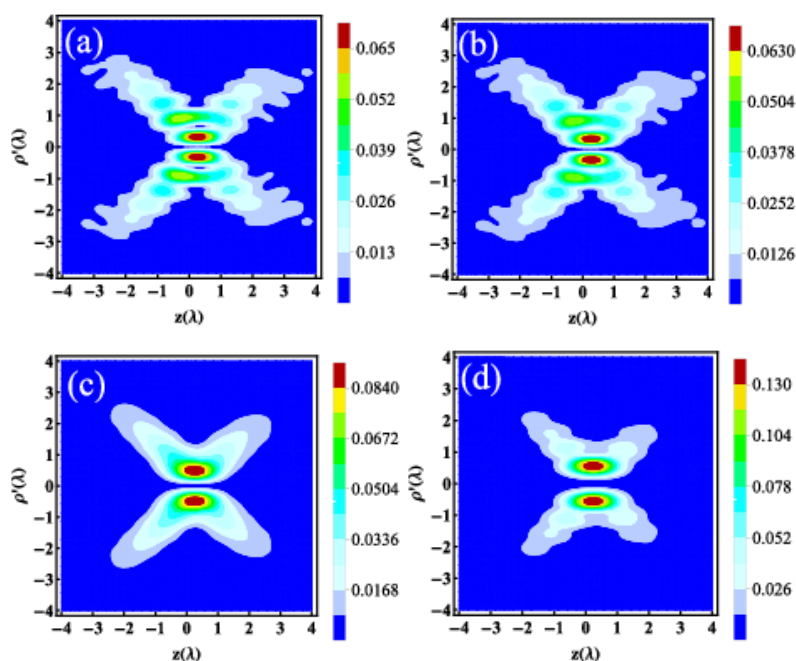


Fig 6. Total intensity distribution of CPVBs in the focal region (a) $\varphi_0=90^\circ$, (b) $\varphi_0=70^\circ$ (c) $\varphi_0=40^\circ$; (d) $\varphi_0=0^\circ$ for $l=2$. The other parameters are the same as those in Fig.2

4. Conclusion

In conclusion, focus shaping of CPVBs by linear axicon is studied numerically by using the vector diffraction theory. It is observed that by tuning the polarization angle, topological charge and the numerical aperture maximal angle different shapes such as focal spot, flat-topped and focal hole are obtained. A longitudinally polarized dark hollow channel and azimuthally polarized dark hollow channel are obtained at focal region when $\varphi_0=0^\circ$ and $\varphi_0=90^\circ$, respectively. Moreover, a flat-topped beam can be obtained by adjusting the value of the polarization rotation angle. The different focal region shapes may find wide applications such as material processing and optical tweezers.

References

- [1] L. Allen, M. W. Beijersbergen, R. Spreeuw, J. Woerdman, Orbital angular momentum of light and the transformation of laguerre-gaussian laser modes, *Physical review A* 45 (11) (1992) 8185. doi: <https://doi.org/10.1103/PhysRevA.45.8185>.
- [2] A. M. Yao, M. J. Padgett, Orbital angular momentum: origins, behavior and applications, *Advances in Optics and Photonics* 3 (2) (2011) 161–204. doi: <https://doi.org/10.1364/AOP.3.000161>.
- [3] M. R. Dennis, K. O'Holleran, M. J. Padgett, Singular optics: optical vortices and polarization singularities, *Progress in optics* 53 (2009) 293–363. [https://doi.org/10.1016/S0079-6638\(08\)00205-9](https://doi.org/10.1016/S0079-6638(08)00205-9)
- [4] A. S. Desyatnikov, L. Torner, Y. S. Kivshar, Optical vortices and vortex solitons, arXiv preprint nlin/0501026 doi: arXiv:nlin/0501026.
- [5] Q. Zhan, Cylindrical vector beams: from mathematical concepts to applications, *Advances in Optics and Photonics* 1 (1) (2009) 1–57. doi: <https://doi.org/10.1364/AOP.1.000001>.
- [6] M. Li, S. Yan, B. Yao, Y. Liang, P. Zhang, Spinning and orbiting motion of particles in vortex beams with circular or radial polarizations, *Optics express* 24 (18) (2016) 20604–20612. doi: <https://doi.org/10.1364/OE.24.020604>.
- [7] M. Chen, S. Huang, W. Shao, Tight focusing of radially polarized circular airy vortex beams, *Optics Communications* 402 (2017) 672–677. doi: <https://doi.org/10.1016/j.optcom.2017.06.089>.
- [8] H. Huang, G. Xie, Y. Yan, N. Ahmed, Y. Ren, Y. Yue, D. Rogawski, M. J. Willner, B. I. Erkmen, K. M. Birnbaum, et al., 100 tbit/s free-space data link enabled by three-dimensional multiplexing of orbital angular momentum, polarization, and wavelength, *Optics letters* 39 (2) (2014) 197–200. doi: <https://doi.org/10.1364/OL.39.000197>.
- [9] A. P. Porfirev, A. V. Ustinov, S. N. Khonina, Polarization conversion when focusing cylindrically polarized vortex beams, *Scientific Report* 6 (1) (2016) 1–9. doi: <https://doi.org/10.1038/s41598-016-0015-2>.
- [10] Z. Xiaoqiang, C. Ruishan, W. Anting, Focusing properties of cylindrical vector vortex beams, *Optics Communications* 414 (2018) 10–15. doi: <https://doi.org/10.1016/j.optcom.2017.12.076>.
- [11] S. N. Khonina, Vortex beams with high-order cylindrical polarization: features of focal distributions, *Applied Physics B* 125 (6) (2019) 1–10. doi: <https://doi.org/10.1007/s00340-019-7212-1>.
- [12] Y. Miao, G. Wang, X. Shan, X. Zeng, Q. Zhang, X. Gao, Focal pattern evolution of azimuthally polarized Lorentz-gaussian vortex beam, *Optik* 187 (2019) 17–24. doi: <https://doi.org/10.1016/j.ijleo.2019.04.070>.
- [13] L. Rao, J. Pu, Z. Chen, P. Yei, Focus shaping of cylindrically polarized vortex beams by a high numerical-aperture lens, *Optics & Laser Technology* 41 (3) (2009) 241–246. doi: <https://doi.org/10.1016/j.optlastec.2008.06.012>.
- [14] T. Wang, C. Kuang, X. Hao, X. Liu, Focusing properties of cylindrical vector vortex beams with high numerical 7 aperture objective, *Optik* 124 (21) (2013) 4762–4765. doi: <https://doi.org/10.1016/j.ijleo.2013.01.070>.
- [15] G. T. Anita, C. A. P. Janet, K. Prabakaran, T. Pillai, K. Rajesh, Effect of spherical aberration on tightly focused cylindrically polarized vortex beams, *Optik* 125 (23) (2014) 6870–6873. doi: <https://doi.org/10.1016/j.ijleo.2014.08.124>.
- [16] G. T. Anita, N. Umamageswari, K. Prabakaran, T. Pillai, K. Rajesh, Effect of coma on tightly focused cylindrically polarized vortex beams, *Optics & Laser Technology* 76 (2016) 1–5. doi: <https://doi.org/10.1016/j.optlastec.2015.07.002>.
- [17] G. Wang, Y. Miao, Q. Zhan, G. Sui, R. Zhang, Focusing of linearly polarized lorentz-gaussian beam with helical axicon, *Optik* 130 (2017) 266–272. <https://doi.org/10.1016/j.ijleo.2016.10.045>
- [18] K. S. Youngworth, T. G. Brown, Focusing of high numerical aperture cylindrical-vector beams, *Optics Express* 7 (2) (2000) 77–87. doi: <https://doi.org/10.1364/OE.7.000077>.
- [19] S. Sato, Y. Kozawa, Hollow vortex beams, *JOSA A* 26 (1) (2009) 142–146. doi: <https://doi.org/10.1364/JOSAA.26.000142>.

Author information

ORCID A. A. AlKelly: [0000-0002-6900-6393](https://orcid.org/0000-0002-6900-6393)Ibrahim G. H. Loqman: [0000-0003-4730-4047](https://orcid.org/0000-0003-4730-4047)Hassan T. Al-Ahsab: [0000-0001-8156-7225](https://orcid.org/0000-0001-8156-7225)

مقالة بحثية

التشكيل البؤري للحزم الحلزونية المستقطبة اسطوانيا بواسطة العدسات المخروطية الخطية

عده احمد الكلي^{1*} , إبراهيم لقمان¹ , حسان ثابت الاحصب^{2,1} 

¹ قسم الفيزياء، كلية العلوم، جامعة صنعاء، صنعاء، اليمن
² قسم الفيزياء، كلية العلوم التطبيقية، جامعة نمار، نمار، اليمن

الباحث الممثل: عده احمد الكلي؛ بريد الكتروني: aa_alkelly@yahoo.com

استلم في: 08 سبتمبر 2021 / قبل في: 27 سبتمبر 2021 / نشر في: 31 ديسمبر 2021

المُلخَص

التشكيل البؤري للحزم الحلزونية أو الملتوية المستقطبة اسطوانيا بواسطة العدسات المخروطية الخطية درس نظريا. استخدمت نظرية الحيود المتجهية لاشتقاق التعبيرات الرياضية للمجال الكهربائي لليزر في منطقة البؤرة. تم الحصول على توزيعات مختلفة للشدة في منطقة البؤرة بواسطة تغيير العدد الكمي للزخم الضوئي وزاوية دوران الاستقطاب والقيمة العظمى لزاوية الفتحة. البقعة البؤرية المضيفة، القناة البؤرية المظلمة والبقعة البؤرية المستوية تم الحصول عليها باختيار قيم مناسبة للبارامترات. تم الحصول أيضا على قناة مظلمة ذات خصائص استقطاب مختلفة قابلة للتحكم في منطقة البؤرة. هذه الأشكال المختلفة لليزر في منطقة البؤرة يمكن استخدامها في تطبيقات الملاقط البصرية ومعالجات المواد بالليزر.

الكلمات المفتاحية: التشكيل البؤري، الاستقطاب، الحزم الحلزونية، العدسة المخروطية الخطية.

How to cite this article:

A. A. AlKelly, Ibrahim G. H. Loqman and Hassan T Al-Ahsab, "FOCUS SHAPING OF CYLINDRICALLY POLARIZED VORTEX BEAMS BY A LINEAR AXICON", *Electron. J. Univ. Aden Basic Appl. Sci.*, vol. 2, no. 4, pp. 145-150, Dec. 2021. DOI: <https://doi.org/10.47372/ejua-ba.2021.4.122>



Copyright © 2021 by the Author(s). Licensee EJUA, Aden, Yemen. This article is an open access article distributed under the terms and conditions of the Creative Commons Attribution (CC BY-NC 4.0) license.